

Star Formation Rates for Elliptical Galaxies Derived from the WISE 12- and 22- μm Emission

(Kadar Penghasilan Bintang untuk Terbitan Galaksi Elips Terbitan daripada Gelombang 12- dan 22- μm WISE)

NUR HIDAYAH MOHD ALI¹, ZAMRI ZAINAL ABIDIN^{1*} & CHORNG-YUAN HWANG²

¹*Physics Department, Universiti Malaya, 50603 Kuala Lumpur, Federal Territory, Malaysia*

²*Graduate Institute of Astronomy, National Central University, Zhong-Li, Taoyuan 32001, Taiwan*

Received: 13 February 2022/Accepted: 22 April 2022

ABSTRACT

We investigated the star formation rates (SFRs) of selected elliptical galaxies using the infrared data from the Wide-field Infrared Survey Explorer (WISE). The elliptical galaxies were selected from the Sloan Digital Sky Survey (SDSS) MPA-JHU catalog and morphology classified by Galaxy Zoo catalog. We used the 3.4- μm emission (W1) of WISE to represent the stellar mass of the galaxies and the 12- and 22- μm emission (W3 and W4) of WISE to represent the star formation activity of the galaxies. The W3- and W4-based star formation rates are usually overestimated due to the star emission in low star-forming galaxies. Stellar continuum emission could contribute to MIR fluxes of elliptical galaxies with an average overestimation of ~ 13.95 and $\sim 0.77\%$ from the observed fluxes of WISE W3 and W4-bands, which determined by using the estimated WISE W3 and W4 flux correction factors. Better SFRs can be obtained by subtracting the stellar contribution of the sources. Our result highlights the possibility of the existence of unknown mechanisms triggering the continuous star formation activities in elliptical galaxies.

Keywords: Galaxies; IR sources; star formation

ABSTRAK

Kami mengkaji kadar penghasilan bintang dalam galaksi elips terpilih menggunakan data inframerah daripada Wide-field Infrared Survey Explorer (WISE). Galaksi dipilih daripada katalog Sloan Digital Sky Survey (SDSS) MPA-JHU dan disaring mengikut bentuk berdasarkan katalog Galaxy Zoo. Gelombang 3.4- μm (W1) daripada WISE digunakan bagi mewakili jisim bintang galaksi dan gelombang 12- and 22- μm (W3 dan W4) mewakili aktiviti penghasilan bintang. Kadar penghasilan bintang berdasarkan W3 dan W4 seringkali dianggarkan lebih tinggi disebabkan isyarat daripada bintang dalam galaksi yang kadar penghasilan bintangnya adalah rendah. Purata lebihan anggaran daripada WISE W3 adalah ~ 13.95 dan W4 adalah $\sim 0.77\%$ bagi galaksi elips, diukur berdasarkan anggaran daripada faktor pembetulan untuk WISE W3 dan W4. Kadar penghasilan binatang yang lebih tepat diperolehi dengan menolak sumbangan daripada bintang tersebut. Keputusan kami menunjukkan bahawa tidak mustahil wujudnya satu mekanisme yang menghasilkan bintang secara berterusan dalam galaksi elips.

Kata kunci: Galaksi; pembentukan bintang; punca inframerah

INTRODUCTION

Star formation rate (SFR) is one of the most important parameters in determining galaxy formation and evolution. The SFR of galaxies is strongly correlated with the morphology of the galaxies along the Hubble sequence. Active star-forming galaxies are normally related to late-type galaxies while non-star forming

galaxies are dominated by early-type galaxies. The study done by Kennicutt et al. (1983) showed that the H- α equivalent width increases along the early-type to late-type galaxies, suggesting that the early-type galaxies are lacking in young, bright stars and star-forming regions.

The study on SFR indicators has been carried out in various frequencies. For example, radio continuum

emission at 1.4 GHz (21 cm) is a good SFR tracer at radio wavelengths (Condon et al. 1992; Murphy et al. 2011; Rieke et al. 2009). Hydrogen recombination emission lines and forbidden lines (H- α and [O_{III}]) are widely used in optical observations. Dust emission at infrared (Hayward et al. 2014; Kennicutt et al. 2012, 1998) and X-ray binary emission (Calzetti et al. 2005; Schmitt et al. 2006) were also commonly used in SFR studies.

Optical lines and UV continuum are widely studied SFR tracers because the emission comes directly from the ionizing photons of young and massive stars. However, these tracers could be strongly affected by dust extinction as most of the star formation takes place in the obscured regions. Thus, infrared observations were performed to trace the star-forming activity as the emission originates from the dust heated by hot and young stars. There have been a number of studies that derived SFR indicators from MIR emission (Calzetti et al. 2007; Helou et al. 2004; Lee et al. 2013; Wu et al. 2005; Zhu et al. 2008). However, those works do not exclude stellar emissions from their derivation, which is the strength of this paper. It is unclear whether these SFR indicators are applicable to galaxies with low star-forming activities. Boselli et al. (2003) showed that the MIR emission of optically selected normal, early-type galaxies are dominated by the Rayleigh-Jeans (R-J) tail of old stellar populations. As a consequence, the contamination from the stellar continuum can severely bias the derivations of SFRs for early-type galaxies using MIR emission.

In this study, we investigated the SFRs of elliptical galaxies selected from the Sloan Digital Sky Survey Max Planck Institute for Astronomy – Johns Hopkins University (MPA-JHU) catalogue (Tremonti et al. 2004). The elliptical galaxies were identified using the Galaxy Zoo morphology parameters (Lintott et al. 2008) and the data were cross-matched with the catalogue of the Wide-field Infrared Survey Explorer (WISE, Wright et al. 2010). We used the WISE 12- and 22- μ m emission to obtain the SFRs of the sources derived from MIR indicators. We adopt the Λ CDM cosmological parameters with $\Omega_m=0.3$, $\Omega_\lambda=0.7$ and $H_0=70$ km s⁻¹ Mpc⁻¹ throughout this paper.

OBSERVATIONAL DATA SDSS AND WISE CROSS-MATCHED DATA

We constructed a sample of galaxies selected from the MPA-JHU value-added galaxy catalogue, (VAGCs). We then matched the galaxies to the WISE objects from the WISE All-Sky Data Release catalogue (Wright et al. 2010).

We choose the galaxies with spectroscopic redshifts within restricted ranges of $0.01 \leq z \leq 0.2$. Thus, this results in 679,342 SDSS-WISE matched galaxies in our primary sample. WISE has mapped the entire sky with four MIR bands centred at 3.4, 4.6, 12, and 22- μ m (hereafter W1, W2, W3, and W4, respectively). Our samples with 3σ detections have been limited to have signal-to-noise ratios ≥ 3 (for all the WISE bands) and have a reliable detection of spectroscopic emission lines of H α and H β . This cut left us with 168,448 galaxies (24.8% of the primary sample).

DATA SELECTION AND DATA REDUCTION

We removed the galaxies with active galactic nuclei (AGN) to avoid the AGN contamination in our samples by determining the optical spectral type based on the Baldwin-Phillips-Terlevich (BPT) diagnostic diagram (Baldwin et al. 1981). We also excluded the broad-line AGN based on spectral identification using the QSO template. In addition, we also removed the broad-line AGN by detecting the candidates of galaxies or quasars that have lines detected at the 10σ level with $\sigma > 200$ km s⁻¹ at the 5σ level. To ensure negligible AGN contamination, we have excluded all the AGN sources that could be enshrouded by dust by limiting the samples to have a WISE colour of $[3.4] - [4.6] < 0.8$ (Vega mag); as AGNs are identified to have $[3.4] - [4.6] \geq 0.8$ mag from MIR colour diagram (Stern et al. 2005). This yielded us with 148,118 galaxies after the AGN colour and emission line cuts.

The above samples were then morphologically classified into the elliptical and spiral galaxy by using the Galaxy Zoo catalogue (Lintott et al. 2011, 2008). To avoid uncertainties in categorizing the samples, we chose the samples with debiased fraction votes ≥ 0.8 for more than 10 voters for both elliptical and spiral classifications. We put another selection criteria for elliptical galaxies by requiring the SDSS parameter $fracDeV \geq 0.9$ from the optical r-band. This parameter represents the bulge fraction in the profile fitting using the de Vaucouleur's 1/4 law. Fulfilling every criterion mentioned above, there are 2,337 elliptical galaxies and 36,842 spiral galaxies in our final galaxy samples.

Besides that, the flux densities for all filters have been corrected for redshift effects based on their spectroscopic redshift. This study involves many star forming ellipticals, which probably cannot be considered as typical galaxies. To avoid any assumption added on the properties of these galaxies, the flux densities from

W1, W3, and W4 filters have been corrected for redshift effects by using linear interpolation and extrapolation of the observed flux densities (Caccianiga et al. 2015). Our computed k-correction value at a specific redshift bin is consistent with a very low variation, ~ 0.02 .

MIR emission could originate from various mechanisms (Da et al. 2008; Draine et al. 2007) including warm dust continuum and polycyclic aromatic hydrocarbons (PAH) emissions (Li et al. 2001; Panuzzo et al. 2011; Rieke et al. 2009; Smith et al. 2007), dust continuum from very small grains (VSGs) (Contursi et al. 2000; Schreiber et al. 2004), AGN heated hot dust continuum (Mullaney et al. 2011; Netzer et al. 2007), and Asymptotic Giant Branch (AGB) circumstellar dust (Bressan et al. 1998, Piovan et al. 2003). To properly measure the star formation activities in the galaxies, the emission of circumstellar dust and AGNs need to be subtracted as they could potentially give an impact on MIR SFRs. In addition, the circumstellar dust emission has been proposed as an age tracer of old stellar populations and showed to be ubiquitous in early-type galaxies (Davis et al. 2014; Simonian et al. 2017; Temi et al. 2007). Simonian et al. (2017) have assumed that these galaxies have no or lesser diffuse, interstellar dust compared to regular dustless galaxies. This effect on the star-forming galaxies (with Specific Star-Formation Rate, SSFR $\sim 10^{-10} \text{ yr}^{-1}$) seems negligible, however, it is more significant in galaxies with relatively little diffuse dust, including low-metallicity and/or non-star forming galaxies (Villaume et al. 2015). This method quantifies the effect of circumstellar dust by using ‘color-cut’ dustless galaxies, which is defined as having $[W1]-[W4] < 1.52 \text{ mag}$ and $[W1]-[W3] < 0.67 \text{ mag}$. Simonian and Martini (2017) have assumed that these galaxies have no or lesser diffuse, interstellar dust compared to regular dustless galaxies. This effect on the star-forming galaxies (SSFR $\sim 10^{-10} \text{ yr}^{-1}$) seems negligible, however, it is more significant in galaxies with relatively little diffuse dust, including low-metallicity and/or non-star forming galaxies (Villaume et al. 2015). The estimated average contribution of AGB circumstellar dust obtained in spiral galaxy samples are $\sim 8.47 \times 10^{-2}$ and $\sim 1.103 \times 10^{-1}$ at 12- and 22- μm , respectively. Meanwhile, this effect shows a quite higher contribution in elliptical galaxy samples, with an average AGB dust contribution ~ 0.45 and ~ 0.32 at 12- and 22- μm , respectively. We have also removed all the AGN-dominated galaxies and those with a tiny sign of AGN activities ($\sim 20,000$ galaxies) based on their optical spectrum features and MIR colour.

RESULTS AND ANALYSIS

WISE SFR INDICATORS

WISE W3 and W4 bands were used as MIR SFR indicators because of the good sensitivity towards the typical features of ongoing star formation such as warm dust and 11.3- μm PAH (Chang et al. 2015; Donoso et al. 2012; Jarrett et al. 2012; Lee et al. 2013; Shi et al. 2012). The MIR emission attributed only from the star-forming regions in the galaxy gives a good correlation between the two SFR indicators. However, there are other factors that can significantly contribute to the MIR spectrum of the source that could overestimate the SFRs. From the galaxy samples described in the previous section, we examined the correlation between SFRs derived from WISE W3 and W4 luminosities using SFRs conversion factor by Lee et al. (2013) and can be refer from equation (1) and (2):

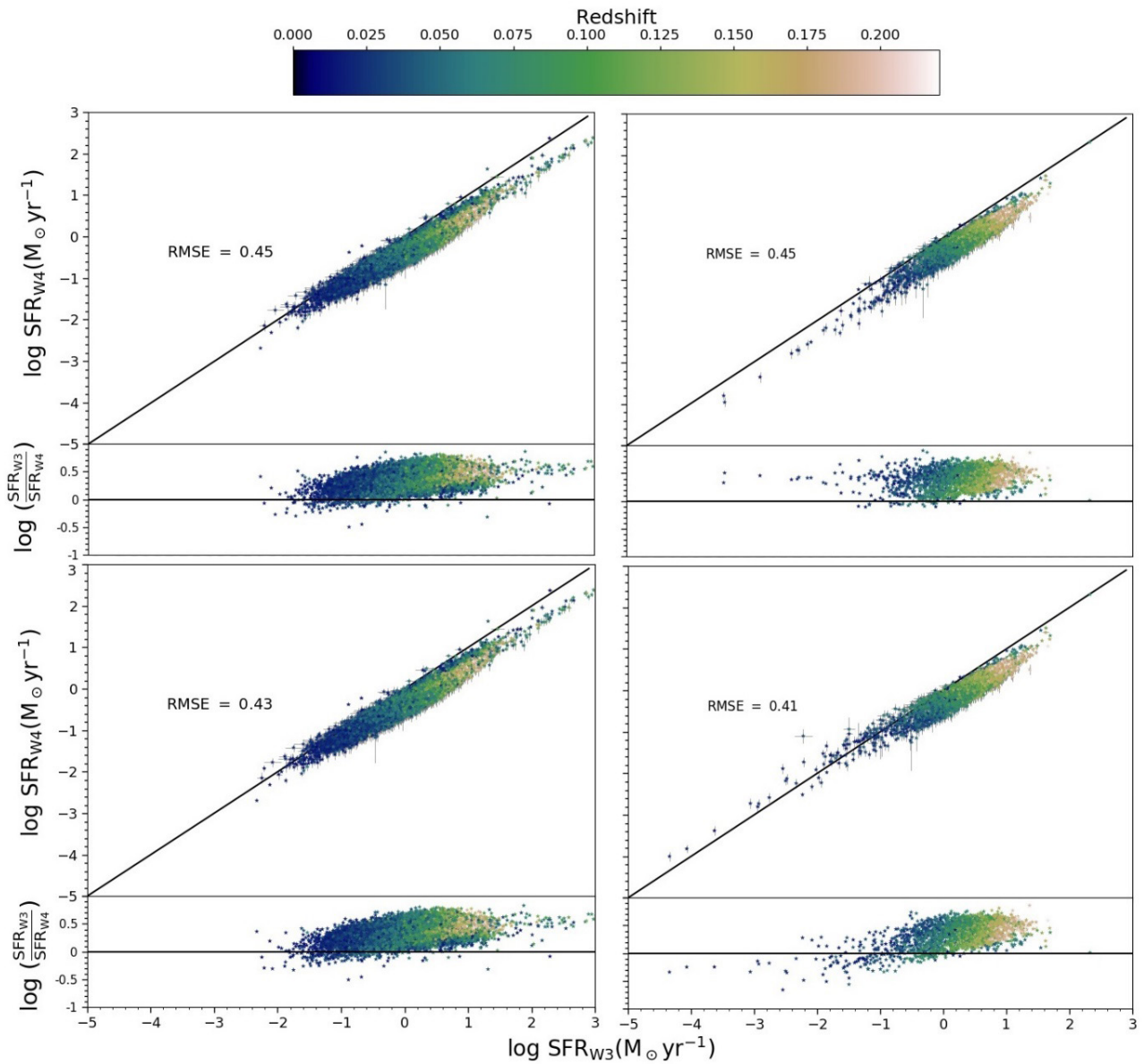
$$\text{SFR}_{W3} (\text{M}_{\odot} \text{ yr}^{-1}) = 9.54 \times 10^{-10} L_{W3}^{1.03} (\text{L}_{\odot}) \quad (1)$$

$$\text{SFR}_{W4} (\text{M}_{\odot} \text{ yr}^{-1}) = 4.25 \times 10^{-9} L_{W4}^{0.96} (\text{L}_{\odot}) \quad (2)$$

The top panels of Figure 1 show the comparison between two WISE SFR indicators, W3 and W4 bands for spiral (left) and elliptical (right) galaxies. The black solid lines indicate the one-to-one relation. The colour scale indicates an increasing redshift covering $0.01 \leq z \leq 0.2$. We also estimated the residuals of each comparison, as shown at the bottom of every plot. As can be seen clearly from Figure 1 (top), both of the WISE SFR indicators show a good correlation. There is also a pattern where most of the data lie just below the one-to-one relationship with an average residual scattering of ~ 0.45 dex for both galaxy morphology classes. This suggests that the SFRs derived by the W3 band are consistently giving a higher value compared to the SFRs derived by the W4 band. There are a few possibilities that can cause this situation; one of them is the stellar continuum emission in the MIR spectrum, which contributes more significantly at the rest-frame of the W3 band but much weaker in the W4 band. We specifically examine this effect in the next subsection.

STELLAR CONTRIBUTION AT 12- AND 22-MM LUMINOSITIES

The existence of an offset in the $\text{SFR}_{W4} - \text{SFR}_{W3}$ relation might be due to the contamination of the other



The solid lines indicate the one-to-one relation. The color-coded shows the spectroscopic redshift of the galaxies. The error bars represent the 1σ uncertainties for the sample

FIGURE 1. Top: comparison between W3-based SFR and W4-based SFR for spiral (left) and elliptical (right) galaxies, and bottom: comparison between the corrected stellar contribution of SFR_{W3} and SFR_{W4} for spiral (left) and elliptical (right) galaxies

components in the MIR SFR indicators. Besides the heat from the old stellar population and AGN activities, the stellar continuum at MIR wavelength could also lead to an overestimation of the true SFRs. The effect of AGN activities and AGB circumstellar dust emission are already considered to be almost negligible in our calibration. In this study, we propose to prevail over the contamination

of stellar contribution by deriving the correction factors at W3- and W4-band. The derivation is estimated from the emission at the WISE W3 and W4 bands relative to the fraction of the stellar continuum at the W1 band. We estimated the stellar correction factors for W3 and W4 bands relative to W1 band (denoted as η_{w3} and η_{w4} by using WISE signal (Wright et al. 2010) as equation (3):

$$\eta_i = \frac{\int R(i) \lambda F_\lambda(i) d\lambda}{\int R(W1) \lambda F_\lambda(W1) d\lambda} \quad (3)$$

where $i = W3$ and $W4$, $R(i)$ is the WISE Relative Spectral Response and λF_λ represents the integrated flux density.

From the calculations, we obtained the average values for W3 and W4 correction factors to be $\eta_{w3} = 0.130 \pm 0.005$ and $\eta_{w4} = 0.010 \pm 0.001$. This bigger value of η_{w3} possibly corresponds to a wider W3 bandpass and closer to the NIR windows, which prominently makes the contribution of the stellar continuum is higher in the W3 compared to the W4 band. The value of stellar correction factor for the W3 band, η_{w3} from this study is comparable to the scaling factors obtained by Jarrett et al. (2012) and Lee et al. (2013), which are ~ 0.15 and ~ 0.1 , respectively. The stellar continuum contributes a higher percentage in the elliptical galaxy samples, which is $\sim 13.95\%$ at the W3 band and $\sim 0.77\%$ at the W4 band. However, in the most extreme cases for the non-star forming elliptical galaxy, the stellar contribution can contribute nearly 89.5 and 10% at W3 and W4 bands, respectively. The W3 emission of these extremities might not be suitable to estimate their star formation rate and they are also excluded from the samples as we derived the SFR later.

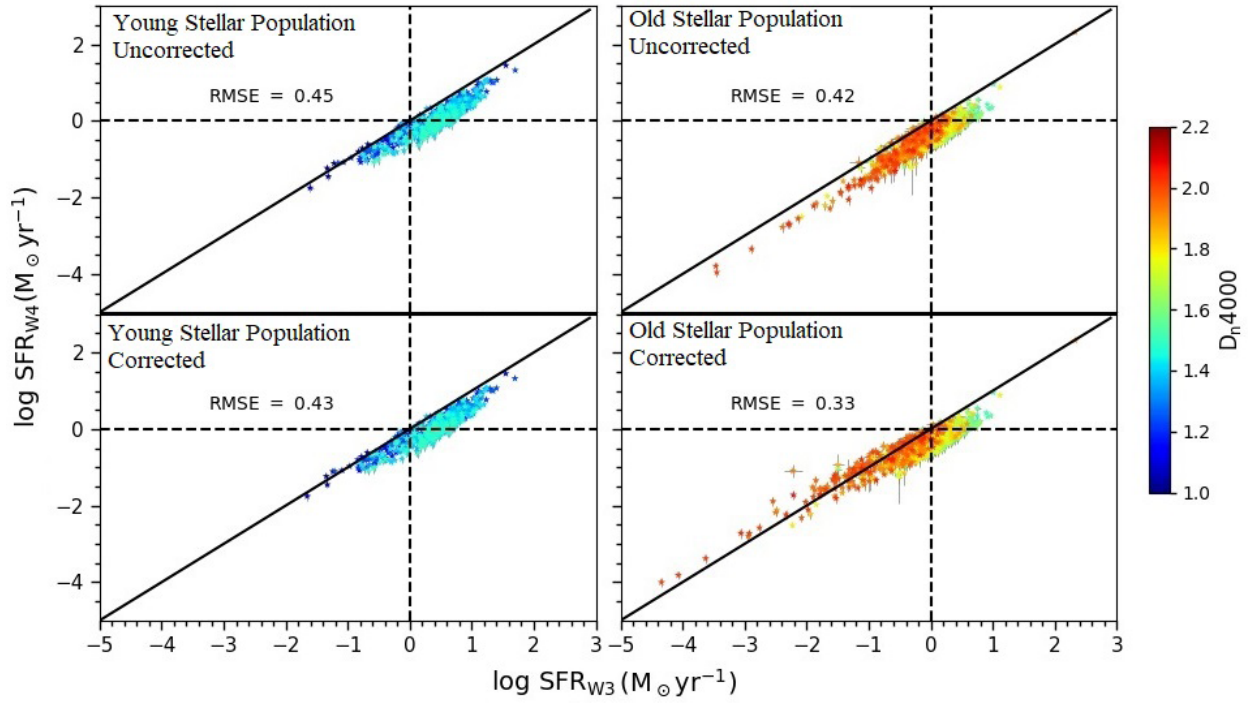
Consequently, we re-examined the correlation of the corrected stellar contribution SFR at 12- and 22- μm (hereafter $\text{SFR}_{W3(\text{corr})}$ and $\text{SFR}_{W4(\text{corr})}$, respectively). This correlation is graphically illustrated in the bottom panels of Figure 1; the left panel for the spirals and right for ellipticals. We then analysed the differences between the uncorrected (top) and corrected (bottom) WISE SFRs for the stellar continuum. First of all, the distribution of the corrected SFRs show almost the same pattern, where most of the data lie just below the one-to-one relation. Nevertheless, the distribution of corrected SFRs show a slightly tight correlation for both spiral and elliptical galaxies with an average overall scatter in the residuals of ~ 0.43 and ~ 0.41 dex, respectively.

For the spiral galaxies, the slope of the SFR relations does not change much after the corrections have been applied. This indicates that the stellar contribution in spiral galaxy is almost insignificant over the redshift range of $0.01 < z < 0.2$. In contrast, the slope of SFR relations for elliptical galaxies has changed significantly after the stellar correction from $m = 0.92$ to $m = 0.8$ and the average offset reduced to ~ 0.41 dex. This change is substantially contributed by the

elliptical galaxies that are located at redshift $z < 0.1$ ($\sim 63.5\%$ from our total elliptical galaxy samples). This population has converged the SFR relation towards the one-to-one relation and shows a smaller offset after we subtracted out the excess stellar contribution. The RMSE for elliptical galaxies at the lower redshift bin ($z < 0.1$) reduced significantly from 0.44 to 0.38 dex, whilst for those at the higher redshift bin ($0.1 < z < 0.2$) only a slight change of RMSE from 0.47 to 0.46 dex is seen. This scenario illustrates that the SFRs for the lower redshift galaxies are more affected by the contamination of the stellar continuum in the MIR spectrum compared to those at higher redshift. Although there may be an uncertainty in the SFR calibration due to metallicity, this is unlikely as our sample is massive ($> 10^{10} M_\odot$).

The D_{4000} spectral index is important to show the significance of subtracting the stellar contribution in elliptical galaxies. This spectral index determines the strength of the 4000 Å breaks, which is used to estimate the mean age of the stellar population in a galaxy (Kauffmann et al. 2003b; Zaritsky et al. 1995). A higher value of D_{4000} index indicates that the galaxy has an abundance of the old stellar population, whereas the younger stellar population in the galaxy gives a smaller index (Kauffmann et al. 2003b; Westra et al. 2010). Brinchmann et al. (2004) shows that most of the star formation process takes place in the galaxy with a low D_{4000} index. The D_{4000} index used in this study is adopted from the SDSS MPA-JHU spectroscopic catalogue with the definition and measurement performed following the Balogh et al. (1999) method.

Referring to Figure 2, we showed that the relationship between the age of the stellar population and the corrected (bottom) and uncorrected (top) WISE SFRs of the elliptical galaxies. The black solid line indicates the one-to-one relation and the dashed line acts as a separator between high star-forming ($\text{SFR} > 1 M_\odot \text{ yr}^{-1}$) and low star-forming galaxies ($\text{SFR} < 1 M_\odot \text{ yr}^{-1}$). We have categorized the elliptical galaxy samples into two distinct populations, where the first one is the galaxy dominated by the young stellar population with $D_{4000} < 1.5$ (left panel) and the second group is the galaxy dominated by the old stellar population with $D_{4000} > 1.5$ (right panel). Noted that the galaxies with the young stellar population have a small offset similar to the spiral galaxies have. Meanwhile, the galaxy population with older stars demonstrates a better correlation between the corrected WISE SFRs. The relation of $\text{SFR}_{W4(\text{corr})} - \text{SFR}_{W3(\text{corr})}$ deviates toward the one-to-one relation and reduces the offset of the relation from ~ 0.42 to ~ 0.33 dex. Specifically, the galaxies that experienced an obvious



The colour coded shows the D4000 indices, the solid line indicates the one-to-one relation and the dashed line is the separator between high and low star-forming galaxies. The error bars represent the 1σ uncertainties for the sample

FIGURE 2. Comparison between the uncorrected (top) and corrected (bottom) stellar contribution of SFRW4-SFRW3 relation for elliptical galaxies with the young stellar population (left) and the old stellar population (right)

change in their corrected SFRs are mostly distributed below the dashed lines. This indicates that the stellar continuum has a highly significant contribution in the elliptical galaxy population that is dominated by the old stellar population with low star-forming activities.

DISCUSSION

Comparisons on WISE-derived SFRs conversion factors have been done between this study and two other

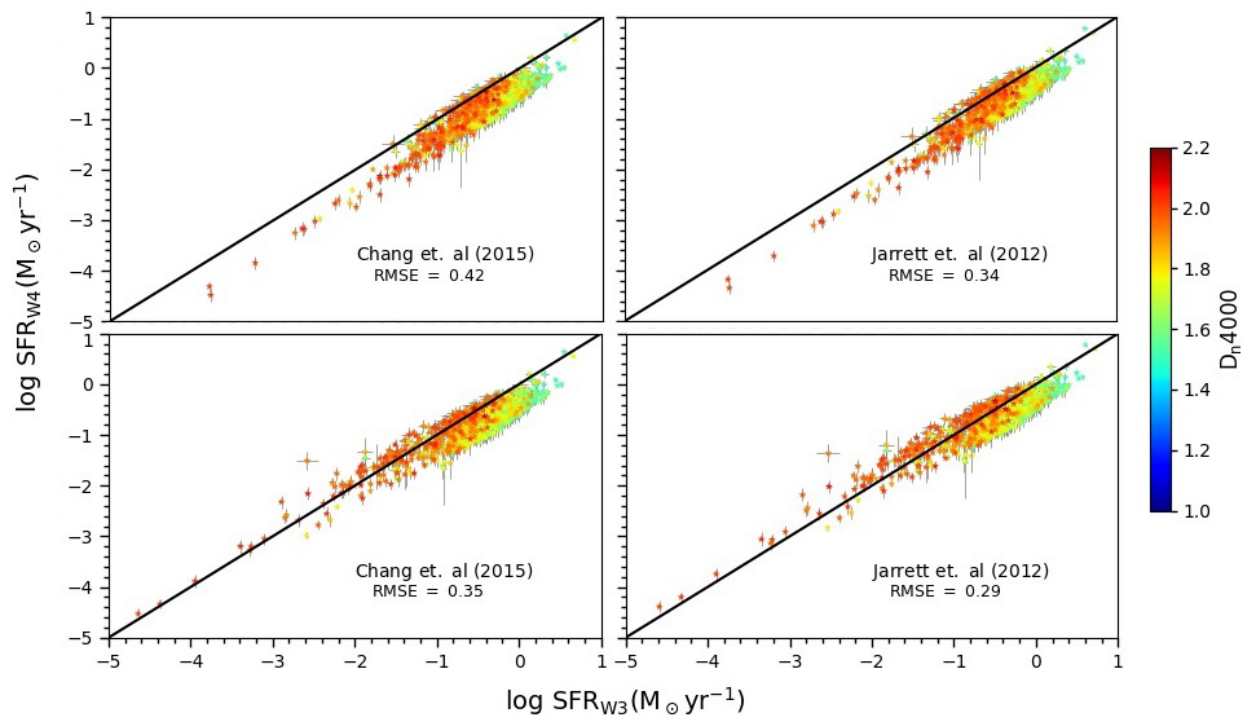
previous studies, Chang et al. (2015) and Jarrett et al. (2012). This is shown in Table 1. Figure 3 shows the comparison of the uncorrected (top) and corrected (bottom) WISE W4 - W3 SFR relations with D_{4000} colour-coded. In Chang's case, the RMS relative to the one-to-one relation changes from ~ 0.42 to ~ 0.35 dex. Meanwhile, for Jarrett, the RMS reduces from ~ 0.34 to ~ 0.29 dex. The reduction in the data scattering shows a better correlation of the corrected SFRs for the old stellar population galaxies in both studies.

TABLE 1. SFR Calibration for WISE W3- and W4-based luminosities

Reference	Jarrett (2012)	Chang (2015)	This study
Sample size	17 well-resolved galaxies	~ 858365	~ 2337
Range of redshift	Nearby (60 Mpc)	Reliable redshift	0.01-0.2
SFR range $M_{\odot} y^{-1}$	0.03 - 4	10^{-3} - 100	10^{-4} - 10^{100}
Morphology	diverse	Star-forming galaxies	Optically classified elliptical galaxies.
Calibrator	24 μ m	UV-MIR SED modelling	H α

The derived correction factors have given out a consistent result even though different approaches were applied in these previous studies to calibrate their SFR formulas. Besides the differences in sample selection, modelling technique also contributes to systematic differences. The calibration carried out by Jarrett et al. (2012) uses the SFRs of GALEX UV fluxes and standard

Spitzer/MIPS 24- μm , which are adopted from Rieke et al. (2009). The conversions done by Lee et al. (2013) are based on the SFRs estimated from H α luminosities. This illustrates that the contribution of the stellar continuum could be significant in the MIR spectrum and strongly signifies that extra caution is needed in the calibration of SFRs using 12- and 22- μm emission.



The solid line represents the one-to-one relation. The error bars represent the 1σ uncertainties for the sample

FIGURE 3. Comparison between the uncorrected (top) and corrected (bottom) stellar contribution of SFRW4-SFRW3 relation derived by Chang et al. (2015) (left) and Jarrett et al. (2012) (right)

CONCLUSION

We have studied a large sample of star-forming galaxies from the SDSS MPA-JHU catalogue with unique matching to the WISE data with MIR detection. Stellar continuum emission could contribute in MIR fluxes of elliptical galaxies with an average overestimation of $\sim 13.95\%$ and $\sim 0.77\%$ from the observed fluxes of WISE W3 and W4-bands, which determined by using the estimated WISE W3 and W4 flux correction factors, $\eta_{w3} = 0.1300.005$ and $\eta_{w4} = 0.0100.001$, respectively, for the galaxies within redshift bin of $0.01 \leq z \leq 0.2$. Low star-forming elliptical galaxy with the old stellar population ($\text{SFR} < 1 M_{\odot} \text{ yr}^{-1}$ and $D_{4000} > 1.5$) gives a good

correlation between SFR_{w3} and SFR_{w4} after the correction of stellar contribution is applied. For the case of the elliptical galaxies with high star-forming and/or young stellar population, stellar contribution seems negligible. Not all star-forming galaxy populations suit the SFRs conversion factors derived in the literature. Their SFRs could be overestimated when applying the SFRs conversion factor, which is derived not specifically for the population.

ACKNOWLEDGEMENTS

This work is supported by the University of Malaya's Faculty of Science Research Grant, GPF081-2020 and

the University of Malaya's High Impact Research Grant UM.S/625/3/HIR/24. Special thanks to Institute of Astronomy, National Central University, Taiwan and all Extragalactic Group members 2015. This publication makes use of data products from the Wide-field Infrared Survey Explorer, which is a joint project of the University of California, Los Angeles, and the Jet Propulsion Laboratory/California Institute of Technology, funded by the National Aeronautics and Space Administration. Funding for the SDSS and SDSS-II was provided by the Alfred P. Sloan Foundation, the Participating Institutions, the National Science Foundation, the U.S. Department of Energy, the National Aeronautics and Space Administration, the Japanese Monbukagakusho, the Max Planck Society, and the Higher Education Funding Council for England. The SDSS was managed by the Astrophysical Research Consortium for the Participating Institutions.

REFERENCES

- Baldwin, J.A., Phillips, M.M. & Terlevich, R. 1981. Classification parameters for the emission-line spectra of extragalactic objects. *Publications of the Astronomical Society of the Pacific* 93(551): 5.
- Balogh, M.L., Morris, S.L., Yee, H.K.C., Carlberg, R.G. & Ellingson, E. 1999. Differential galaxy evolution in cluster and field galaxies at $z \approx 0.3$. *The Astrophysical Journal* 527(1): 54.
- Boselli, A., Sauvage, M., Lequeux, J., Donati, A. & Gavazzi, G. 2003. Mid-IR emission of galaxies in the Virgo cluster III. The data. *Astronomy & Astrophysics* 406(3): 867-877.
- Bressan, A., Granato, G.L. & Silva, L. 1998. Modelling intermediate age and old stellar populations in the infrared. *Astronomy and Astrophysics* 332: 135-148.
- Brinchmann, J., Charlot, S., White, S.D.M., Tremonti, C., Kauffman, G., Heckman, T. & Brinkmann, J. 2004. The physical properties of star-forming galaxies in the low-redshift Universe. *Monthly Notices of the Royal Astronomical Society* 351(4): 1151-1179.
- Caccianiga, A., Antón, S., Ballo, L., Foschini, L., Maccacaro, T., Ceca, R.D., Severgnini, P., Marchã, M.J., Mateos, S. & Sani, E. 2015. WISE colours and star formation in the host galaxies of radio-loud narrow-line Seyfert 1. *Monthly Notices of the Royal Astronomical Society* 451(2): 1795-1805.
- Calzetti, D., Kennicutt, R.C., Engelbracht, C.W., Leitherer, C., Draine, B.T., Kewley, L., Moustakas, J., Sosey, M., Dale, D.A., Gordon, K.D. & Helou, G.X. 2007. The calibration of mid-infrared star formation rate indicators. *The Astrophysical Journal* 666(2): 870.
- Calzetti, D., Kennicutt Jr., R.C., Bianchi, L., Thilker, D.A., Dale, D.A., Engelbracht, C.W., Leitherer, C., Meyer, M.J., Sosey, M.L., Mutchler, M. & Regan, M.W. 2005. Star formation in NGC 5194 (M51a): The panchromatic view from GALEX to Spitzer. *The Astrophysical Journal* 633(2): 871.
- Chang, Y., van der Wel, A., da Cunha, E. & Rix, H. 2015. Stellar masses and star formation rates for 1 m galaxies from sdss+ wise. *The Astrophysical Journal Supplement Series* 219(1): 8.
- Condon, J.J. 1992. Radio emission from normal galaxies. *Annual Review of Astronomy and Astrophysics* 30(1): 575-611.
- Contursi, A., Lequeux, J. & Cesatsky, C. 2000. Mid-infrared imaging and spectrophotometry of N 66 in the SMC with ISOCAM. *Astronomy and Astrophysics* 362: 310-324.
- Da Cunha, E., Charlot, S. & Elbaz, D. 2008. A simple model to interpret the ultraviolet, optical and infrared emission from galaxies. *Monthly Notices of the Royal Astronomical Society* 388(4): 1595-1617.
- Davis, T.A., Young, L.M., Crocker, A.F., Bureau, M., Blitz, L., Alatalo, K., Emsellem, E., Naab, T., Bayet, E., Bois, M. & Bournaud, F. 2014. The ATLAS3D Project—XXVIII. Dynamically driven star formation suppression in early-type galaxies. *Monthly Notices of the Royal Astronomical Society* 444(4): 3427-3445.
- Donoso, E., Yan, L., Tsai, C., Eisenhardt, P., Stern, D., Assef, R.J., Leisawitz, D., Jarrett, T.H. & Stanford, S.A. 2012. Origin of 12 μ m emission across galaxy populations from WISE and SDSS surveys. *The Astrophysical Journal* 748(2): 80.
- Draine, B.T. & Li, A. 2007. Infrared emission from interstellar dust. IV. The silicate-graphite-PAH model in the post-Spitzer era. *The Astrophysical Journal* 657(2): 810.
- Hayward, C.C., Lanz, L., Ashby, M.L.N., Fazio, G., Hernquist, L., Martínez-Galarza, J.R., Noeske, K., Smith, H.A., Wuyts, S. & Zezas, A. 2014. The total infrared luminosity may significantly overestimate the star formation rate of quenching and recently quenched galaxies. *Monthly Notices of the Royal Astronomical Society* 445(2): 1598-1604.
- Helou, G., Roussel, H., Appleton, P., Frayer, D., Stolovy, S., Storrie-Lombardi, L., Hurt, R., Lowrance, P., Makovoz, D., Masci, F. & Surace, J. 2004. The anatomy of star formation in NGC 300. *The Astrophysical Journal Supplement Series* 154(1): 253.
- Jarrett, T.H., Masci, F., Tsai, C.W., Petty, S., Cluver, M.E., Assef, R.J., Benford, D., Blain, A., Bridge, C., Donoso, E. & Eisenhardt, P. 2012. Extending the nearby galaxy heritage with wise: First results from the wise enhanced resolution galaxy atlas. *The Astronomical Journal* 145(1): 6.
- Kauffmann, G., Heckman, T.M., White, S.D., Charlot, S., Tremonti, C., Peng, E.W., Seibert, M., Brinkmann, J., Nichol, R.C., SubbaRao, M. & York, D. 2003. The dependence of star formation history and internal structure on stellar mass for 105 low-redshift galaxies. *Monthly Notices of the Royal Astronomical Society* 341(1): 54-69.

- Kennicutt, R.C. 1998. The global Schmidt law in star-forming galaxies. *The Astrophysical Journal* 498(2): 541.
- Kennicutt, R.C. & Evans, N.J. 2012. Star formation in the Milky Way and nearby galaxies. *Annual Review of Astronomy and Astrophysics* 50: 531-608.
- Kennicutt, R.C. & Kent, S.M. 1983. A survey of H-alpha emission in normal galaxies. *The Astronomical Journal* 88: 1094-1107.
- Lee, J.C., Ho, S.H. & Ko, J. 2013. The calibration of star formation rate indicators for WISE 22 μ m-selected galaxies in the Sloan Digital Sky Survey. *The Astrophysical Journal* 774(1): 62.
- Li, A. & Draine, B.T. 2001. Infrared emission from interstellar dust. II. The diffuse interstellar medium. *The Astrophysical Journal* 554(2): 778.
- Lintott, C.J., Schawinski, K., Slosar, A., Land, K., Bamford, S., Thomas, D., Raddick, M.J., Nichol, R.C., Szalay, A., Andreescu, D. & Murray, P. 2008. Galaxy zoo: Morphologies derived from visual inspection of galaxies from the Sloan Digital Sky Survey. *Monthly Notices of the Royal Astronomical Society* 389(3): 1179-1189.
- Lintott, C., Schawinski, K., Bamford, S., Slosar, A., Land, K., Thomas, D., Edmondson, E., Masters, K., Nichol, R.C., Raddick, M.J. & Szalay, A. 2011. Galaxy Zoo 1: Data release of morphological classifications for nearly 900 000 galaxies. *Monthly Notices of the Royal Astronomical Society* 410(1): 166-178.
- Mullaney, J.R., Alexander, D.M., Goulding, A.D. & Hickox, R.C. 2011. Defining the intrinsic AGN infrared spectral energy distribution and measuring its contribution to the infrared output of composite galaxies. *Monthly Notices of the Royal Astronomical Society* 414(2): 1082-1110.
- Murphy, E.J., Chary, R.R., Dickinson, M., Pope, A., Frayer, D.T. & Lin, L. 2011. An accounting of the dust-obscured star formation and accretion histories over the last ~ 11 billion years. *The Astrophysical Journal* 732(2): 126.
- Netzer, H., Lutz, D., Schweitzer, M., Contursi, A., Sturm, E., Tacconi, L.J., Veilleux, S., Kim, D.C., Rupke, D., Baker, A.J. & Dasyra, K. 2007. Spitzer quasar and ULIRG evolution study (QUEST). II. The spectral energy distributions of Palomar-green quasars. *The Astrophysical Journal* 666(2): 806.
- Panuzzo, P., Rampazzo, R., Bressan, A., Vega, O., Annibali, F., Buson, L.M., Clemens, M.S. & Zeilinger, W.W. 2011. Nearby early-type galaxies with ionized gas-VI. The Spitzer-IRS view. Basic data set analysis and empirical spectral classification. *Astronomy & Astrophysics* 528: A10.
- Piovan, L., Tantaló, R. & Chiosi, C. 2003. Shells of dust around AGB stars: Effects on the integrated spectrum of single stellar populations. *Astronomy & Astrophysics* 408(2): 559-579.
- Rieke, G.H., Alonso-Herrero, Weiner, B.J., Pérez-González, P.G., Blaylock, M., Donley, J.L. & Marcillac, D. 2009. Determining star formation rates for infrared galaxies. *The Astrophysical Journal* 692(1): 556.
- Schreiber, N.M.F., Roussel, H., Sauvage, M. & Charmandaris, V. 2004. Warm dust and aromatic bands as quantitative probes of star-formation activity. *Astronomy & Astrophysics* 419(2): 501-516.
- Schmitt, H.R., Calzetti, D., Armus, L., Giavalisco, M., Heckman, T.M., Kennicutt, R.C., Leitherer, C. & Meurer, G.R. 2006. Ultraviolet-to-far-infrared properties of local star-forming galaxies. *The Astrophysical Journal* 643(1): 173.
- Shi, F., Kong, X., Wicker, J., Chen, Y., Gong, Z.Q. & Fan, D.X. 2012. Star formation rate indicators in Wide-Field Infrared Survey preliminary release. *Journal of Astrophysics and Astronomy* 33(2): 213-220.
- Simonian, G.V. & Martini, P. 2017. Circumstellar dust, PAHs and stellar populations in early-type galaxies: Insights from GALEX and WISE. *Monthly Notices of the Royal Astronomical Society* 464(4): 3920-3936.
- Smith, J.D.T., Draine, B.T., Dale, D.A., Moustakas, J., Kennicutt Jr., R.C., Helou, G., Armus, L., Roussel, H., Sheth, K., Bendo, G.J. & Buckalew, B.A. 2007. The mid-infrared spectrum of star-forming galaxies: Global properties of polycyclic aromatic hydrocarbon emission. *The Astrophysical Journal* 656(2): 770.
- Stern, D., Eisenhardt, P., Gorjian, V., Kochanek, C.S., Caldwell, N., Eisenstein, D., Brodwin, M., Brown, M.J., Cool, R., Dey, A. & Green, P. 2005. Mid-infrared selection of active galaxies. *The Astrophysical Journal* 631(1): 163.
- Temi, P., Brighenti, F. & Mathews, W.G. 2007. Far-infrared Spitzer observations of elliptical galaxies: Evidence for extended diffuse dust. *The Astrophysical Journal* 660(2): 1215.
- Tremonti, C.A., Heckman, T.M., Kauffmann, G., Brinchmann, J., Charlot, S., White, S.D., Seibert, M., Peng, E.W., Schlegel, D.J., Uomoto, A. & Fukugita, M. 2004. The origin of the mass-metallicity relation: Insights from 53,000 star-forming galaxies in the Sloan Digital Sky Survey. *The Astrophysical Journal* 613(2): 898.
- Villaume, A., Conroy, C. & Johnson, B.D. 2015. Circumstellar dust around AGB stars and implications for infrared emission from galaxies. *The Astrophysical Journal* 806(1): 82.
- Westra, E., Geller, M.J., Kurtz, M.J., Fabricant, D.G. & Dell'Antonio, I. 2009. Evolution of the H α luminosity function. *The Astrophysical Journal* 708(1): 534.
- Wright, E.L., Eisenhardt, P.R., Mainzer, A.K., Ressler, M.E., Cutri, R.M., Jarrett, T., Kirkpatrick, J.D., Padgett, D., McMillan, R.S., Skrutskie, M. & Stanford, S.A. 2010. The Wide-Field Infrared Survey Explorer (WISE): Mission description and initial on-orbit performance. *The Astronomical Journal* 140(6): 1868.
- Wu, H., Cao, C., Hao, C., Liu, F., Wang, J., Xia, X., Deng, Z. & Young, C.K. 2005. PAH and mid-infrared luminosities as measures of star formation rate in Spitzer first look survey galaxies. *The Astrophysical Journal Letters* 632(2): L79.

Zaritsky, D., Zabludoff, A.I. & Willick, J.A. 1995. Spectral classification of galaxies along the hubble sequence. *Astronomical Journal* 110: 1602.

Zhu, Y., Wu, H., Cao, C. & Li, H. 2008. Correlations between mid-infrared, far-infrared, H α , and FUV luminosities for Spitzer SWIRE field galaxies. *The Astrophysical Journal* 686(1): 155.

*Corresponding author; email: zzaa@um.edu.my